Modified spontaneous emission from erbium-doped photonic layer-by-layer crystals

M. J. A. de Dood* and A. Polman
FOM Institute for Atomic and Molecular Physics, Kruislaan 407, 1098 SJ Amsterdam, The Netherlands

J. G. Fleming
Sandia National Laboratories, P.O. Box 5800, Albuquerque, New Mexico 87185
(Received 11 December 2002; published 12 March 2003)

The spontaneous emission from luminescent Si photonic layer-by-layer crystals is studied. Luminescence from both implanted Er ions and the polycrystalline Si host is observed in the 1.1–1.7 μm wavelength range and serves as a probe of the photonic band structure. The spontaneous emission is strongly suppressed for wavelengths between 1.4 and 1.7 μm. The spectral changes are described by a model that takes into account changes in the local density of states, internal Bragg scattering in the crystal, and the internal quantum efficiency of the optical transition involved. A spectral attenuation of ~ 5 dB per unit cell is derived from the spontaneous emission data, consistent with theory and transmission data.

DOI: 10.1103/PhysRevB.67.115106 PACS number(s): 42.70.Qs, 42.50.−p

A photonic crystal is a three-dimensional (3D) arrangement of dielectric material that is periodic on a length scale comparable to the wavelength of light and that interacts strongly with light. Photonic crystals can be used to control spontaneous emission and manipulate optical modes in ways that were impossible so far. A major challenge in photonic crystal design and fabrication is to realize a photonic crystal with a full photonic band gap, i.e., a structure in which the propagation of light within a well-defined frequency range is forbidden in any direction in the crystal. This requires, on the one hand, the use of materials with sufficient refractive index contrast and, on the other hand, a well-chosen crystal symmetry. In the past few years, intense research has focused on the fabrication of photonic crystals for optical wavelengths either by using self-assembly and infiltration[1,2] or high-resolution lithography.[3–5] Crystals made by self-assembly, if infiltrated with Si, show a presumed complete photonic band gap at near-infrared wavelengths.[6,7] Lithographic techniques can be applied directly to high-index materials such as Si or GaAs that are needed to obtain a full photonic band gap and structures with a band gap around 1.5 μm were demonstrated in both Si (Refs. 3 and 4) and GaAs (Ref. 5). The use of lithographic tools leads to large crystals in two dimensions while the third dimension is limited to several crystal lattice units.

Although both routes to photonic crystal fabrication are now well developed, the challenge is to demonstrate the existence of a full photonic band gap. So far, optical characterization of photonic crystals with a presumed full photonic band gap mostly involved optical reflectivity and transmission measurements as a function of the external angle of incidence.[4,5,7] The full photonic band structure cannot be obtained from these measurements, since not all propagation directions inside the crystal are accessible by an external probe. However, spontaneous emission from optical probes inside the crystal can probe all possible directions and can be used to explore the properties of crystals that do not have a complete band gap.[8,9] In a true three dimensional photonic crystal, no emission should be detected in any direction. In crystals with a partial gap or in thin crystals that are not truly three-dimensional spontaneous emission can be observed and can thus provide important information on the band structure as well as on the local optical density of states (DOS).

In this article we present data on modified spontaneous emission from finite-thickness (five-layer) Si photonic layer-by-layer crystals. Due to its finite thickness, optical emission from both well-defined atomic-scale defects that are intrinsic to the polycrystalline Si base material and of optically active Er ions that are implanted into the photonic crystal can be observed. A detailed analysis reveals that both ordinary Bragg reflections and the quantum efficiency of the emitting species play an essential role in understanding the luminescence spectra from photonic crystals. Even though it is extremely important, the effect of quantum efficiency is often neglected, most likely because it is unknown *a priori* in an experiment.

The photonic crystals are made by lithography following the layer-by-layer design.[3,10] A polycrystalline (p-Si) layer is deposited by low-pressure chemical vapor deposition from silane at 570 °C. Subsequent annealing at 1040 °C converts any amorphous silicon to p-Si. A one-dimensional array of 180-nm-wide and 200-nm-high polycrystalline Si (p-Si) bars at a repeat distance of 650 nm is etched in the p-Si layer using a fillet process.[3] After completion of the first layer of bars, the structure is filled with SiO_2 and planarized by chemical mechanical polishing. Next, a second layer of Si bars is defined on top, rotated by 90°. This process is repeated until a structure with 5 layers (2.5 primitive unit cells) is formed, as indicated in Fig. 1. After completion of the structure the SiO_2 is removed by wet chemical etching.

Band structure calculations for an infinite Si layer-by-layer crystal show a large band gap (relative bandwidth $\Delta\lambda/\lambda \approx 20\%$).[10] Optical transmission measurements on comparable crystals show that the transmission attenuates by 6 dB per unit cell at 1.5 μm.[4] These results were confirmed by calculations that also reveal that emission from the structure is strongly modified compared to free space.[11] This makes the present five-layer crystals ideal to study photonic

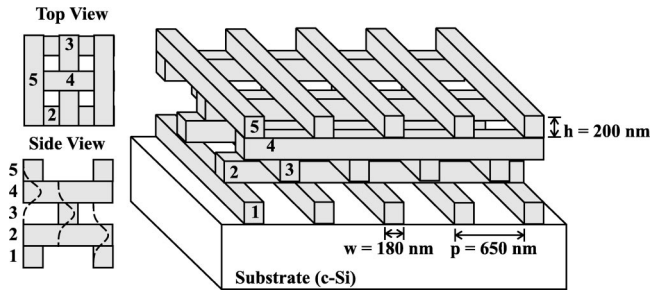

FIG. 1. Schematic 3D drawing of the layer-by-layer lattice showing the stacking of the 5 layers (2.5 primitive unit cells) of *p*-Si bars. Top and side views of the structure are shown as well. The depth of the Er (O) implantation is indicated by the Gaussian-shaped curves in the side view.

crystal properties, as a strong interaction with light is achieved, while some light can still escape from the crystal.

Here 915 keV Er ions were implanted into the layer-by-layer crystal at normal incidence to a dose of 1.5×10^{13} Er cm^{-2}. To activate the Er, oxygen was coimplanted to overlap the Er distribution (Er:O ratio 1:10). The projected range and straggle (σ) of the Er ions are 300 nm and 80 nm, respectively. The Er is thus implanted in the second layer it encounters looking from the top. As a consequence all Er ions are implanted through the top layer and end up in the second, third, and fourth layers. The Er distribution is sketched in Fig. 1 (side view). Part of the erbium (45%) is implanted directly in the crystalline Si (*c*-Si) substrate. However, given the large attenuation, at $\lambda = 1.5$ μm, Er luminescence from this depth will not be detected in our optical measurements. A planar *p*-Si sample was implanted together with the layer-by-layer crystal and serves as a reference. The sample consists of a 2-μm-thick *p*-Si layer on top of a 1 μm-thick Si_3N_4 layer on a *c*-Si substrate.

After implantation all samples were annealed at 600 °C for 3 h under vacuum ($p \leqslant 5 \times 10^{-7}$ mbar), followed by a rapid thermal anneal at 1000 °C for 60 s in a N_2 ambient. Photoluminescence (PL) measurements were taken from samples cooled to 12 K in a closed-cycle He cryostat. As a pump source, 10 mW of 488 nm radiation from an Ar ion laser was focused to a 1 mm spot. The angle of incidence was 20° off the surface normal, and the beam was modulated on-off at a frequency of 20 Hz using an acousto-optic modulator. The luminescence was collected in a cone with a full angle of ~20° (solid angle 10 msr) by a lens, focused on the entrance slits of a 48 cm grating monochromator and detected by a liquid-nitrogen-cooled Ge detector (time response 30 μs).

Figure 2(a) shows measured PL spectra at 12 K from both the implanted layer-by-layer lattice (——) and the *p*-Si reference sample (—×—). Measurements using either the 457 or the 514.5 nm line of the Ar ion laser resulted in identical PL spectra. A sharp peak at $\lambda = 1.1$ μm is visible and corresponds to optical transitions from the indirect electronic band gap of silicon. The broad luminescence band extending from 1.1 μm to well beyond 1.7 μm is attributed to defect-related optical transitions in the *p*-Si host material mediated by recombination of electron-hole pairs. Superimposed on the defect band, a sharp peak at $\lambda = 1.539$ μm is observed due to the $^4I_{13/2} \rightarrow {}^4I_{15/2}$ intra-4*f* transitions of implanted Er ions. The broad luminescence band is observed in unimplanted samples and in samples implanted to different Er and O concentrations and is therefore not related to ion implantation or to erbium or oxygen. Experiments on the same structure performed at temperatures up to 125 K show an overall decrease in PL intensity, which is attributed to thermalization of trapped carriers responsible for the luminescence of the *p*-Si. However, the ratio in PL intensity as shown in Fig. 2(b) was found to be unaltered.

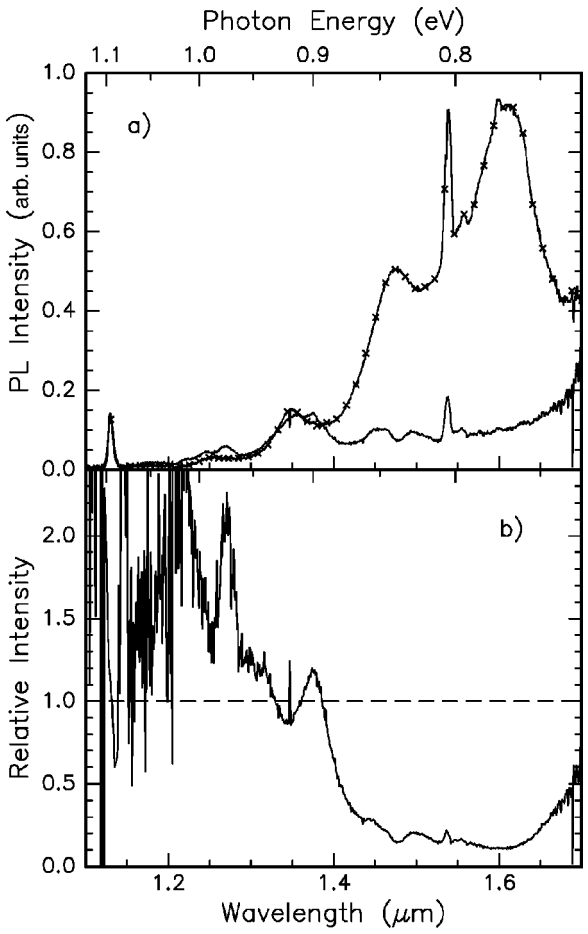

FIG. 2. (a) PL spectra measured at $T = 10$ K of an Er-implanted photonic crystal (——) and the *p*-Si reference sample (—×—). (b) Relative intensity from the photonic crystal compared to the reference sample. A clear dip in the relative intensity is observed in the spectral range 1.4–1.7 μm showing that the emission is suppressed due to the presence of a stop band.

The two spectra shown in Fig. 2(a) are taken at the same pump power and were not normalized. As can be seen, the PL intensity collected from the two samples is comparable for wavelengths shorter than 1.4 μm, while for longer wavelengths much less intensity is collected from the layer-by-layer structure than from the *p*-Si reference. Figure 2(b) shows the intensity ratio of the layer-by-layer and the *p*-Si reference emission and shows a broad dip in the range from 1.4 to 1.7 μm. This broad depression is clearly indicative of

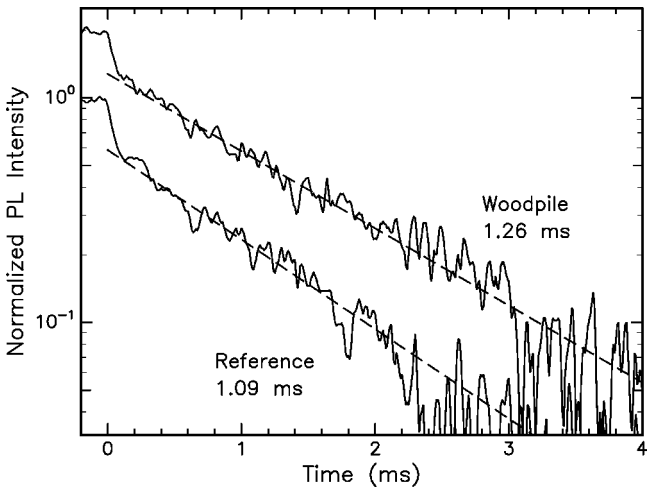

FIG. 3. Photoluminescence decay traces of the layer-by-layer sample and the reference sample. Decay traces were measured at 10 K at the peak wavelength of the Er luminescence ($\lambda = 1.536\ \mu$m). The luminescence shows an initial fast decay related to the defect emission and a slow component related to luminescence from erbium ions embedded in the *p*-Si.

a photonic stop band. The spectral range of the dip is similar to that found in optical transmission and reflection measurements[4,3,12,13] on the same crystal. It is in perfect agreement with calculations of the emissivity spectrum of an electrical dipole in a finite-thickness layer-by-layer lattice.[11] As can be seen, spectral features at wavelengths of 1.27 μm, 1.35 μm, and 1.38 μm are observed in the ratio. These may possibly be related to variations in the (local) DOS at these wavelengths.

The intensity ratio in Fig. 2(b) is determined by the photonic band gap as well as by the distribution of the 488 nm Ar pump laser light in the structure. The pump power distribution in the reference sample decays exponentially in the *p*-Si because of the large absorption of Si at 488 nm (absorption length $\sim 1\ \mu$m). At the pump wavelength light can propagate in the photonic crystal since no band gap is present at that wavelength. As the Si is strongly absorbing, most of the light is directly absorbed in the photonic crystal. This pumping mechanism explains the intensity ratio close to unity outside the band gap region, since the areal density of *e-h* pairs generated (by optical absorption of laser light) is comparable for the photonic crystal and reference samples.

The sharp luminescence peak at $\lambda = 1.536\ \mu$m in both spectra in Fig. 2(a) is related to intra-$4f$ transitions of Er^{3+}. The Er emission collected from the photonic crystal is strongly suppressed compared to that of the reference sample. Interestingly, the ratio between the spectra in Fig. 2(b) shows a small Er related peak. This indicates that the effect of the photonic crystal on the Er ions is different than the effect on the defect luminescence. In the remainder of this paper this will be discussed in more detail by combining the data in Fig. 2 with luminescence lifetime measurements.

PL decay traces taken at the peak of the erbium emission ($\lambda = 1.536\ \mu$m) are plotted in Fig. 3. The decay traces for both the reference sample and the layer-by-layer structure show an initial fast decay limited by the detector response time, followed by a slow component. Lifetime measurements at different wavelengths indicate that the fast component is related to the defect luminescence, while the slow component is related to the Er emission. Moreover, the ratio between fast and slow components matches the ratio between defect and Er luminescence at 1.536 μm observed in the spectra in Fig. 2(a). The slow component can be described by a single-exponential decay with lifetimes of 1.09 ms and 1.26 ms ($W = 920 \pm 50\ s^{-1}$ and $790 \pm 50\ s^{-1}$) for the reference and photonic crystal samples, respectively.

The data clearly demonstrate that spontaneous emission is affected by the photonic band gap of the layer-by-layer lattice. The effect is twofold. First, radiation emitted from within a crystal can Bragg reflect which leads to a dip in the spectra over the stop band region. This effect is present in any photonic crystal and does not require a complete photonic band gap. The second effect is a modification of the spontaneous emission rate and becomes important if a significant amount of the entire 4π solid angle is blocked by Bragg reflection. In fact, even if the band gap is incomplete, the DOS can be strongly reduced and spontaneous emission be partly inhibited. To evaluate the exact effect of the photonic crystal on the spontaneous emission rate both the position of the optical probe and the local DOS must be evaluated.[14]

For any luminescent species, the total PL emitted over all directions depends on the radiative rate W_{rad} and the steady-state population of luminescing species. The steady-state population depends on the pump rate and total decay rate W_{tot}. For a two-level system in the low-pump-power limit the total PL intensity is given by

$$I_{PL} \propto R_{pump} \frac{W_{rad}}{W_{tot}} N, \tag{1}$$

where R_{pump} denotes the excitation rate, N is the total number of excitable species, and W_{rad}/W_{tot} equals the internal quantum efficiency (QE) of the optical transition. Both the Er and defect luminescence in Fig. 2 can be described using this two-level model. Next, the effect of (Bragg) diffraction, which lowers the collected intensity, must be included. Defining the fraction of light collected from the structure as η, the ratio in PL intensity (I_{PC}/I_{ref}) [see Fig. 2(b)] from the photonic crystal (PC) and the reference sample can be expressed as

$$\frac{I_{PC}}{I_{ref}} = \frac{W_{rad,PC}}{W_{rad,ref}} \frac{W_{tot,ref}}{W_{tot,PC}} \frac{\eta_{PC}}{\eta_{ref}}, \tag{2}$$

where $W_{rad,PC}$ ($W_{rad,ref}$) and $W_{tot,PC}$ ($W_{rad,ref}$) denote the radiative and total decay rates of the emitting species in the PC (reference) sample and η_{PC} and η_{ref} are the collection efficiencies of the luminescence from the PC and reference sample, respectively. Note that Eq. (2) holds for both the defect luminescence and the Er luminescence separately. This equation includes three important parameters that determine changes in the spontaneous emission collected from a photonic crystal: (1) changes in W_{rad} due to changes in the

(local) DOS, (2) the quantum efficiency of the optical transition involved, and (3) a collection efficiency and Bragg reflection effect.

The importance of the quantum efficiency in Eq. (2) is obvious; in practical studies, however, it is often neglected, most often because it is unknown. Two extreme cases may be considered: For unit QE ($W_{rad}=W_{tot}$), the observed ratio in PL intensity is η_{PC}/η_{ref} and is thus determined by Bragg reflection only. On the other hand, if the QE is very small ($W_{tot,ref}\approx W_{tot,PC}$), the ratio in PL intensity equals ($W_{rad,PC}/W_{rad,ref}$) (η_{PC}/η_{ref}) and does contain the effect of the DOS on the radiative lifetime as well. This counterintuitive result is due to the fact that for transitions with high QE a reduced W_{rad} will cause a higher steady-state excited population in the crystal, whereas for transitions with low QE it will not.

With this model the data in Fig. 2(b) can be analyzed quantitatively. First the intrinsic *p*-Si defect luminescence is analyzed. Defect-related transitions in Si are generally nonradiative in nature, and therefore the QE for radiative emission is very small. From the data we can thus estimate ($W_{rad,PC}/W_{rad,ref}$) (η_{PC}/η_{ref})$=0.13$, the measured defect PL intensity ratio at $\lambda=1.536$ μm. The relative contribution of defect and Er luminescence at this wavelength was derived from the fast and slow components observed in the decay traces in Fig. 3. By using the measured total decay rates from Fig. 3, the Er luminescence can be treated similarly. Using Eq. (2) and the measured data for W_{tot} we obtain a value of ($W_{rad,PC}/W_{rad,ref}$) (η_{PC}/η_{ref})$=0.23$. The fact that this number differs from that found for the defect luminescence may be related to a difference in the depth distribution of luminescing species, which affects both η and W_{rad} (through the local DOS).

This analysis does not determine the factor ($W_{rad,PC}/W_{rad,ref}$), which would directly give the modification of the spontaneous emission rate of Er by the photonic crystal. Assuming a radiative rate of Er in Si of 500 ± 100 s^{-1} ($\tau=2$ ms) (Ref. 15) (being, to our knowledge, the longest lifetime of Er in Si), we deduce a nonradiative rate of $\sim 420\pm110$ s^{-1} in the reference sample ($W_{tot,ref}=920$ s^{-1}). This nonradiative decay is likely related to direct energy transfer from erbium to electronic states in the *p*-Si host and is thus equal in the reference and PC sample. Subtracting the nonradiative rate from the measured total decay rate, a radiative rate of $\sim 370\pm110$ s^{-1} (790–420) for the PC is found. This value is suppressed by $25\%\pm10\%$ compared to the reference sample. The spontaneous emission from an infinite layer-by-layer crystal of the dimensions used in our experiment should be fully suppressed at $\lambda=1.536$ μm (DOS = 0). The fact that this is not the case is attributed to the finite size of the crystal. To compare this number to theoretical results requires knowledge of the Er depth distribution and the local DOS in the finite-thickness photonic crystal.[16,17]

Finally, using the value found for ($W_{rad,PC}/W_{rad,ref}$) (370/500), we evaluate that for the Er emission $\eta_{PC}/\eta_{ref}=0.3$ (5 dB). This number represents the reduced emission from the crystal due to Bragg reflection and can be compared to transmission measurements as a function of crystal thickness[4,11] that report a reduction in the transmission of ~ 6 dB per primitive unit cell (= 2 layers). The erbium ions are implanted in the third layer (implantation depth = 300 nm), leaving two layers on top, in good agreement with the found value of 5 dB.

In conclusion, spontaneous emission from an Er-implanted Si photonic layer-by-layer crystal is strongly modified relative to emission from a planar reference sample. Both the Er^{3+} emission at 1.535 μm and the intrinsic defect emission from the polycrystalline Si are strongly reduced in the stop band (1.4–1.7 μm). The spectral modifications are due to (1) changes in spontaneous emission rate (through the local density of states) and (2) changes in the light collection due to Bragg scattering in the crystal. Using a rate equation argument it is shown that, depending on the quantum efficiency of the optical transition, only the latter or both of these effects must be taken into account. The spontaneous emission rate of Er at 1.53 μm was found to be reduced by $25\%\pm10\%$ and a spectral attenuation of ~ 5 dB per primitive cell is found, consistent with theory and transmission measurements. These measurements are the first demonstration of modified spontaneous emission from a Si photonic crystal at the important telecommunication wavelength of 1.5 μm.

The silicon photonic lattices were fabricated at Sandia National Laboratories' Microelectronics Development Laboratory (MDL). The process and design was guided by Dr. Shawn-Yu Lin, also of Sandia National Laboratories. Sandia is a multiprogram laboratory operated by Sandia Corporation, a Lockheed Martin Company, for the United States Department of Energy under Contract No. DE-AC04-94AL85000. This work is part of the research program of the Foundation for Fundamental Research on Matter (FOM) and was made possible by financial support from the Dutch Organization for Scientific Research (NWO).

*Corresponding author. Present address: California Nanosystems Institue, University of California Santa Barbara, Santa Barbara, CA 93106. Electronic address: mdedood@physics.ucsb.edu

[1] D. J. Norris and Y. A. Vlasov, Adv. Mater. **13**, 371 (2001) and references therein.
[2] J. E. G. J. Wijnhoven and W. L. Vos, Science **281**, 802 (1998).
[3] J. G. Fleming and S.-Y. Lin, Opt. Lett. **24**, 49 (1999).
[4] S.-Y. Lin *et al.*, Nature (London) **394**, 251 (1998).
[5] S. Noda, K. Tomoda, N. Yamamoto, and A. Chutinan, Science **289**, 604 (2000).
[6] A. Blanco *et al.*, Nature (London) **405**, 437 (2000).
[7] Y. A. Vlasov, X.-Z. Bo, J. C. Sturm, and D. J. Norris, Nature (London) **71**, 289 (2001).
[8] M. Megens, J. E. G. J. Wijnhoven, A. Lagendijk, and W. L. Vos, J. Opt. Soc. Am. B **16**, 1403 (1999).
[9] A. F. Koenderink, L. Bechger, H. P. Schriemer, A. Lagendijk, and W. L. Vos, Phys. Rev. Lett. **88**, 143 903 (2002).
[10] K. M. Ho, C. T. Chan, C. M. Soukoulis, R. Biswas, and M.

Sigalas, Solid State Commun. **89**, 413 (1994).
[11] D. M. Whittaker, Opt. Lett. **25**, 779 (2000).
[12] S.-Y. Lin and J. G. Fleming, IEEE J. Lightwave Technol. **17**, 1944 (1999).
[13] M. J. A. de Dood, B. Gralak, A. Polman, and J. G. Fleming, Phys. Rev. B **67**, 035322 (2003).
[14] R. Sprik, B. A. van Tiggelen, and A. Lagendijk, Europhys. Lett. **35**, 265 (1996).
[15] R. Serna *et al.*, J. Appl. Phys. **79**, 2658 (1996).
[16] T. Suzuki and P. K. L. Yu, J. Opt. Soc. Am. B **12**, 570 (1995).
[17] Z.-Y. Li, L.-L. Lin, and Z.-Q. Zhang, Phys. Rev. Lett. **84**, 4341 (2000).